African Journal of Pure & Applied Sciences

ISSN: 2710-0758
DOI 10.33886/ajpas.v4i3.425

Journal homepage: http://journal.ku.ac.ke/index.php/AJPAS

Research Article Open Access

# Positron and Electron Impact Elastic Scattering by Atomic Beryllium

**Wechuli W.B.[1*], Waswa V. E[2], Linturi J. M.[3], Kariuki P. K.[4]**

[1*,2,4]Department of Physics, Kenyatta University; P.O. BOX 43844-0100, Nairobi, Kenya
[3]Department of Physical Sciences, South Eastern Kenya University; P.O. BOX 170-90200, Kitui, Kenya
[1*]Corresponding Author Email: benardwakhu@gmail.com

**Received 20th August , 2023/ Accepted 18th October 2023, Published online 31st December, 2023**

**How to cite:**
Wechuli, W., Waswa, V., Linturi, J., & Kariuki, P. (2023). Positron and Electron Impact Elastic Scattering by Atomic Beryllium. *African Journal of Pure and Applied Sciences*, 4(3), a-b. https://doi.org/10.33886/ajpas.v4i3.425

## ABSTRACT

Theoretical results for positron and electron elastic scattering from beryllium atom at incident energies ranging from the first inelastic threshold to 200 eV are presented. Elastic, total, momentum transfer, and differential cross sections are computed using both the first order distorted wave Born approximation and the optical potential approaches utilizing a complex potential. We have shown that our data agree fairly well with the available data and provided the details of the Physics in case of discrepancies. This study demonstrates the importance of accurate atomic elastic scattering cross sections.

**Keywords:** Positronium, elastic scattering, cross sections, distorted wave Born approximation

## INTRODUCTION

Understanding the complexities of projectile-target interaction and collision process dynamics entails a consciousness of the elastic scattering of projectiles by atomic targets. Atomic beryllium is an overwhelmingly favorite material for coating the walls of fusion plasma reactors due to its low atomic number (Reid and Wadehra, 2020 and references therein). Additionally, walls with beryllium coatings offer excellent heat conductivity for use in magnetic fusion applications and scattering from a thin beryllium window is crucial process in electron accelerators (Wisniewski *et al.*, 2015).

Despite these practical applications, not much is known about the interactions of atomic beryllium with either electrons or their antiparticles. Accurate cross sections for electron and positron scattering by atomic beryllium are thus of current interest.

Because of their low positronium (Ps) formation threshold, atoms of group two elements offer an intriguing set of targets. For beryllium, the ionization potential $\approx 2.523$ eV above the binding energy of a positronium (6.8 eV). Not much research has been done on electron- and positron-beryllium collisions (Singh *et al.*, 2018). Nonetheless, several approaches including optical potential (Reid and Wadehra, 2020) relativistic polarized orbital approximation (Szmytkowski, 1993), R-matrix (Zatsarinny and Bartschat, 2013) and convergent close-coupling (Fursa and Bray, 2012; Savage *et al.*, 2011; Utamuratov *et al.*, 2012) methods have been applied to calculate cross sections of both electron and positron impact.

## THEORETICAL METHODOLOGY

Distorted Wave Born Approximation (DWBA) is a theoretical technique in Scattering Theory in which the alteration of the field owing to scattering events is thought to be minimal. The DWBA transition matrix (T-matrix) element is expressed:

$$T_{i0}^{DWBA} = T_{i0}^{D1} + T_{i0}^{D2} - T_{i0}^{E} \qquad (1)$$

where $T_{i0}^{D1}$ and $T_{i0}^{D2}$ are the first and second direct terms while $T_{i0}^{E}$ is the exchange T- matrix element; and are respectively given in computational form as:

$$T_{i0}^{D1} = -\frac{1}{4\pi^2} f(\theta) \tag{2}$$

where $f(\theta)$ is the elastic scattering amplitude.

$$T_{i0}^{D2} = -\left[4(\pi k)^2\right]^{-1} \sum_{l=0}^{\infty}(2l+1)e^{2i\delta_l}\left\{P_l(\cos\theta)\int_0^{\infty}\left[\chi_l(k,r)\overline{U}(r)\chi_l(k,r)\right]dr\right\} \tag{3}$$

where $\overline{U} = \left[U_{st}(r) - U_{opt}(r,\mathrm{E})\right]$ is the reduced residual potential.

The exchange T-matrix element is approximated by;

$$T_{i0}^{E} = \left[2(\pi k)^2\right]^{-1} \sum_{l=0}^{\infty}\sum_{n_\beta l_\beta}\sum_{\lambda=|l-l_\beta|}^{l+l_\beta} e^{2i\delta_l}\left[l_\beta\right]l^2\begin{pmatrix} l & \lambda\, l_\beta \\ 0 & 0\;0 \end{pmatrix}^2 R_{\ln_\beta}^{\lambda} P_l(\cos\theta) \tag{4}$$

In the OP method, the transition matrix is expressed as:

$$T_{i0}^{OP} = T_{i0}^{D1} \tag{5}$$

where $T_{i0}^{D1}$ is given by equation (2). The positron can be distinguished from atomic electrons hence the:

i) real part of equation (6) does not contain the potential given by equation (9), and

ii) DWBA T-matrix (equation 1) does not contain the third term given by equation (4).

In the present study, the interaction potential, $U_{opt}(r,\mathrm{E})$, is taken in an approximate form as:

$$U_0 = U_i = U_{opt}(r,\mathrm{E}) = U_{real} + iU_{abs}(r,\mathrm{E}) \tag{6}$$

Where: (i) $U_{real} = U_{st}(r) + U_{ex}(r,\mathrm{E}) + U_{pol}(r,\mathrm{E})$ for electron scattering, and

(ii) $U_{real} = U_{st}(r) + U_{pol}(r,\mathrm{E})$ for positron scattering.

The radial wavefunctions of beryllium calculated and tabulated by (Bunge *et al.*, 1993) have been utilized in evaluating the complex optical potential. The radial distorted (partial) waves, $\chi_l(k,r)$, which are elastic scattering wave functions from the target, satisfy the radial Schrödinger equation

$$\left[\frac{d^2}{dr^2} - \frac{l(2l+1)}{r^2} - U_{opt}(r,\mathrm{E}) + k^2\right]\chi_l(k,r) = 0. \tag{7}$$

## Distorting potentials

The complex potential consists of static, exchange, polarization and absorption potentials; each of these distorting potentials account for a particular physical effect of electron- and positron-atomic beryllium scattering. The local static potential is given by:

$$U_{st}(r)=\frac{Zq}{r}-q\sum_{n_a l_a}2(2l_a+1)\int_0^\infty dr'\frac{p_{n_a l_a}^2(r')}{r_>} \quad (8)$$

where $Z=4$ while $q=-1$ for electron and $q=+1$ for positron scattering. The exchange potential for electron scattering is given by (Furness and McCarthy, 1973)

$$U_{ex}(r,\mathrm{E})=\frac{1}{2}\left\{(\mathrm{E}-U_{st}(r))-\left[(\mathrm{E}-U_{st}(r))^2+4\pi\rho(r)\right]^{1/2}\right\}. \quad (9)$$

In equation (9), $\rho(r)$ is the electronic charge density of the target atom

$$\rho(r)=\sum_{nl}2(2l+1)\frac{p_{nl}^2(r)}{4\pi r^2}. \quad (10)$$

The polarization potential is described by a long range and attractive potential (for both positron and electron) whose magnitude is dependent on the polarizability of the target's electron cloud (Khare *et al*., 1985). The absorption potential of Staszewska *et al*. (1983) as modified by (Wechuli *et al*., 2022) was applied to account for absorption effects.

$$U_{abs}(r,\mathrm{E})=\frac{V_I(r,\mathrm{E})}{k} \quad (11)$$

where $k=\sqrt{2\mathrm{E}}$ is the momentum wave vector and $V_I(r,\mathrm{E})$ is the local absorption potential of Staszewska *et al*. (1983) which is given as:

(i) $V_I(r,\mathrm{E})=-\frac{1}{2}T_{loc}(r,\mathrm{E})\rho(r)\overline{\sigma_b}$ for electron scattering, and

(ii) $V_I(r,\mathrm{E})=-T_{loc}(r,\mathrm{E})\rho(r)\overline{\sigma_b}$ for positron scattering in which the factor of one-half has been replaced by one to account for absence of exchange effects.

where $\rho(r)$ is the electronic charge density of the target atom, the local kinetic energy of the incident projectile

$T_{loc}(r,\mathrm{E})=\sqrt{2(\mathrm{E}-U_{se})}$ with $U_{se}=U_{st}(r)+U_{ex}(r,\mathrm{E})$ and $U_{se}=U_{st}(r)$ respectively for electron and positron

scattering while $\overline{\sigma_b}$ is as given by Staszewska *et al*. (1983). In this paper, we have applied the Chiari *et al*. (2012) absorption threshold given as:

$$\Delta_1=\Delta_e-(\Delta_e-\Delta_p)\exp\left[-(\mathrm{E}-\Delta_p)/\mathrm{E}_m\right] \quad (12)$$

where for beryllium atom $\Delta_e=5.830$ eV, $\Delta_p=2.523$ eV, $\mathrm{E}$ is the projectile's energy and $\mathrm{E}_m=20$ eV.

**Cross Sections**

The differential cross section is given as:

$$\frac{d\sigma}{d\Omega}=(2\pi)^4\frac{k_i}{k_0}\left|\mathrm{T}_{i0}\right|^2 \quad (13)$$

The total inelastic (absorption) cross section, $(\sigma_{abs})$, whose value depends only on, $U_{abs}(r, \mathrm{E})$, as given in equation (11), is same for both OP and DWBA methods and given herein as:

$$\sigma_{abs} = \frac{\pi}{k^2} \sum_{l=o}^{\infty} (2l+1)\left(1-e^{-4\beta_l}\right) \tag{14}$$

The total cross section, $(\sigma_T)$, is given by the optical theorem:

$$\sigma_T = -\left(\frac{2}{k_0}\right)(2\pi)^3 \operatorname{Im} \mathrm{T}_{00} \tag{15}$$

Using equations (14) and (15), the OP as well as the DWBA elastic cross section is given as:

$$\sigma_{el} = \sigma_T - \sigma_{abs} \tag{16}$$

And since this work is based on calculation of phase shifts, $\delta$, the momentum transfer cross section is given by:

$$\sigma_{mtcs} = \frac{4\pi}{k^2} \sum_{l=0}^{\infty} (l+1) \sin^2 (\delta_l - \delta_{l+1}) \tag{17}$$

## RESULTS AND DISCUSSION

### Electron_Beryllium differential cross sections

The present DWBA and OP, each with a complex potential, DCS results are respectively represented by DWBA_Present and OP_Present. The OP results of Reid and Wadehra with a complex potential are represented by R and W (2020) while those of Kaushik *et al.* (1983) with a real potential is denoted by K *et al.*

At 3.0 eV (fig. 1(a)), the models agree well within an increasing deviation of $\pm 3.2\%$ for forward scattering from the scattering angle $\theta \leq 40^{\circ}$. The existing difference between the present and the R and W (2020) model is occasioned by use of different values of $d$ ; the parameter that avoids singularity at $r = 0$ in the Khare *et al.* (1983) polarization potential. Nonetheless, in all the three approximation models, a single prominent minimum occurs at $\theta \approx 110^{\circ}$. The position of the local minimum in DCS shifts toward forward scattering angles, broadens with increasing projectile-target impact energy and is expected to disappear after a certain limit.

At 5.0 eV (fig. 1(b)), the present DWBA and OP results are congenial save for the fact that the later slightly underestimates the former at the position of the local minimum which occurs at $\theta \approx 110^{\circ}$. This is not unexpected since DWBA T-matrix contains an extra direct and exchange terms respectively given herein by equations (3) and (4). The K *et al.* results generally overestimate the present models by $\approx 7.6\%$ for $\theta \leq 50^{\circ}$. This is because K *et al.* utilized a real potential (static, polarization and exchange) thus did not account for absorption effects.

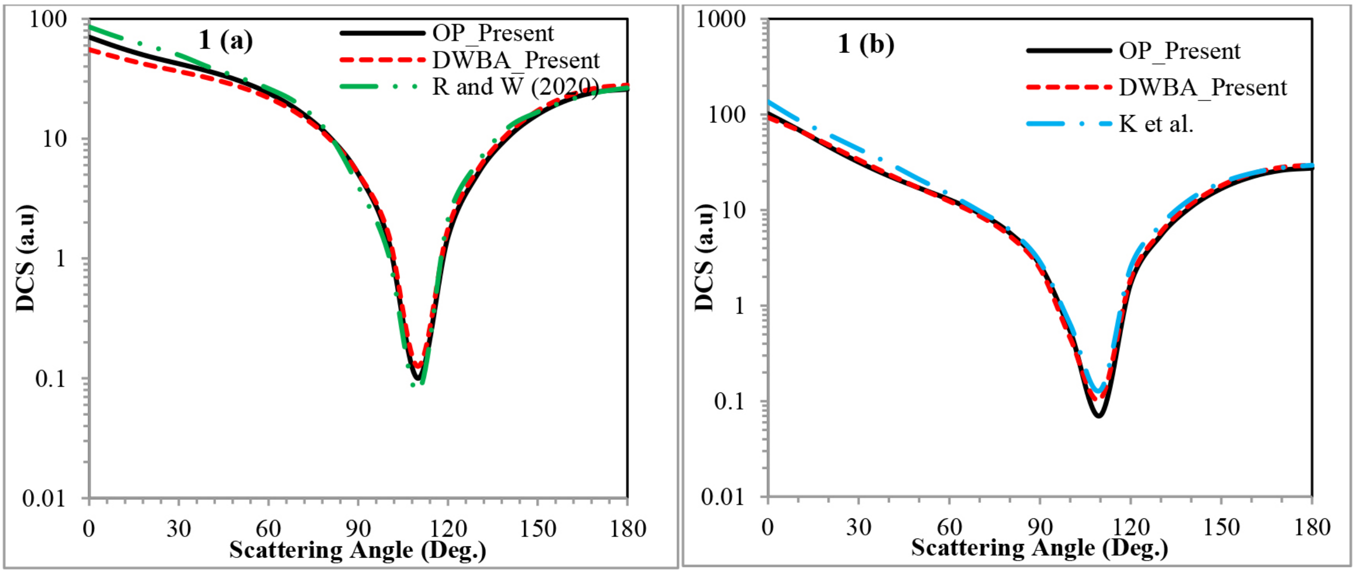


**Fig. 1(a)**: Differential cross sections for electron_beryllium atom elastic scattering at 3.0 eV: DWBA_ and OP_Present; R and W (2020) – Reid and Wadehra, 2020 DCS results each with a complex potential. **Fig. 1(b)**: same as figure 1(a) but at 5.0 eV and K *et al.* – Kaushik *et al.* (1983) with a real potential.

At 10 eV (fig. 1(c)), DWBA and OP the results agree well except at the position of the local minimum. The cause of this discrepancy is already explained herein above. The K *et al.* results overestimates the present results at scattering angle $\theta \leq 50^{\circ}$; which phenomenon is already accounted for. The local minimum shifts to $\theta \approx 90^{\circ}$. At 20 eV (fig 1(d)), a broader local minimum occurs at $\theta \approx 70^{\circ}$. At scattering angle $130^{\circ} \leq \theta \leq 180^{\circ}$, all the three approximations yield results that tend to merge into one. This implies that as the impact energy increases, the cross sections are not so much dependent on the scattering angles.

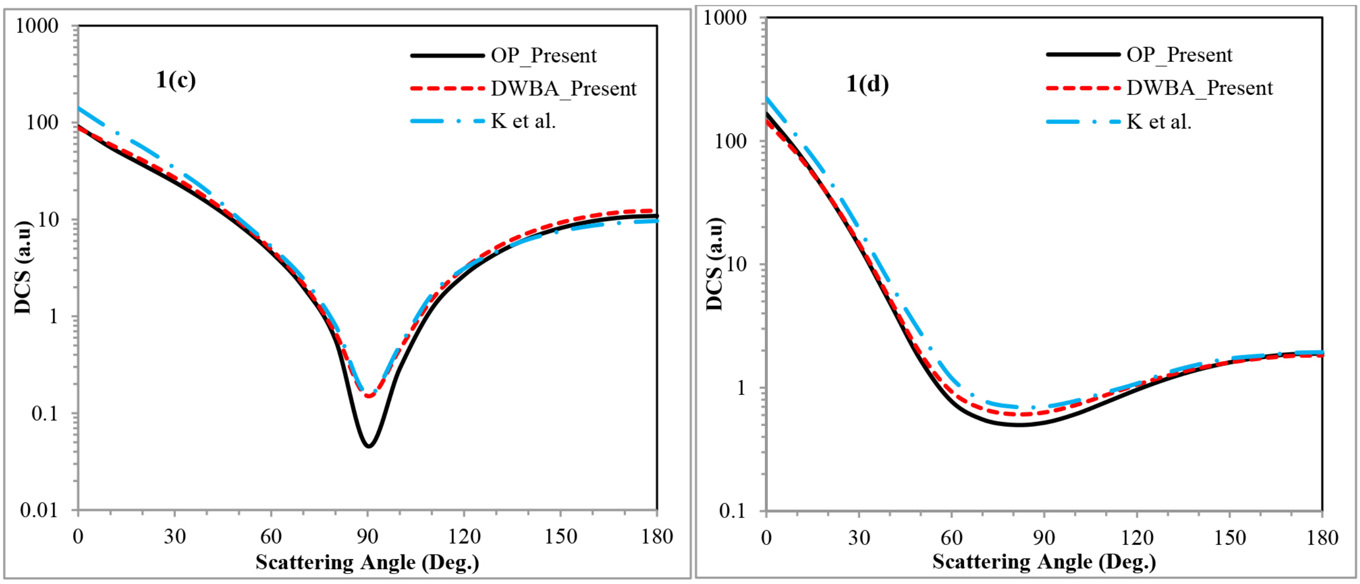


**Figures 1 (c)** and **1 (d)** : Same as **Fig. 1 (b)** but respectively at 10.0 eV and 20.0 eV

## Positron_Beryllium differential cross section

The present first order distorted wave Born and the optical potential models, each with a complex potential, are respectively denoted by DWBA and OP.

At 10 eV (fig. 2(a)), the prominent local minimum occurs at $\theta = 20^{\circ}$ and $\theta = 30^{\circ}$ respectively for DWBA and OP models. The OP results overestimate the DWBA results by $\approx 13.94\%$ for $\theta \leq 25^{\circ}$. Leaving out the other components of the interaction potential, the residual potential contains both the repulsive-static and attractive-polarization potentials, the effects of which typically cancel out, resulting in relatively low DWBA DCS values for small scattering angles.

At 15.0 eV (fig. 2(b)), the local minimum occurs at $\theta = 18^{\circ}$ and $\theta = 20^{\circ}$ respectively for DWBA and OP models. With increasing projectile impact energy, the precise location of the local minimum shifts to lower scattering angles. This phenomenon is consistent with the Classical Physics theory of interference and diffraction, which states that as projectile energy increases, the associated de Broglie wavelength decreases and the interference pattern shifts to smaller scattering angles.

At 20.0 eV (fig. 2(c)), the local minimum occurs at $\theta = 15^{\circ}$ and $\theta = 18^{\circ}$ respectively for DWBA and OP models. The difference in DCS results up to around the position of the local minimum has already been explained herein.

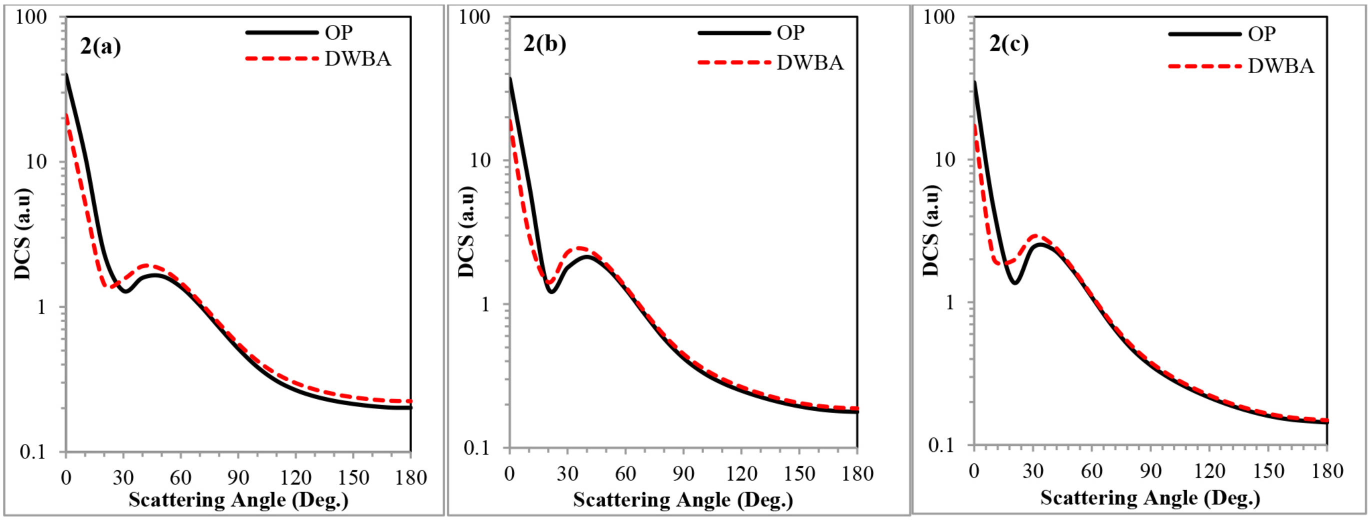


**Fig. 2(a):** Differential cross sections for positron_beryllium atom elastic scattering at 10.0 eV: DWBA and OP DCS results each with a complex potential. **Fig. 2(b)** and **2(c)**: Same as **Fig. 2(a)** but respectively at 15.0 eV and 20.0 eV

At 30.0 eV (fig. 2(d)), the local minimum occurs at $\theta \approx 12^{\circ}$ for both approximations. The magnitude of the difference in DCS up to around the position of the local minimum has significantly reduced. Further, the DCS values have reduced due to low contribution of the quadrupole term in the polarization potential. At 100.0 eV (fig. 2(e)), the local minimum occurs at $\theta \approx 8^{\circ}$ for both approximations. The depths of the minima have significantly reduced. These minima are introduced in the DCS structures once the polarization potential is incorporated into the interaction potential. This behavior is not unexpected since the polarization potential utilized in this study is energy-dependent hence its effect is anticipated to vanish at very high incident projectile's energy. At 200.0 eV (fig. 2(f)), with rising scattering angles, the DCS values fall rapidly, resulting in a distinctive virtually structureless curve. This behavior is expected since at such high impact energy, from Classical Physics point of view, the large forward momentum of the incident projectile dominate the scattering effects.

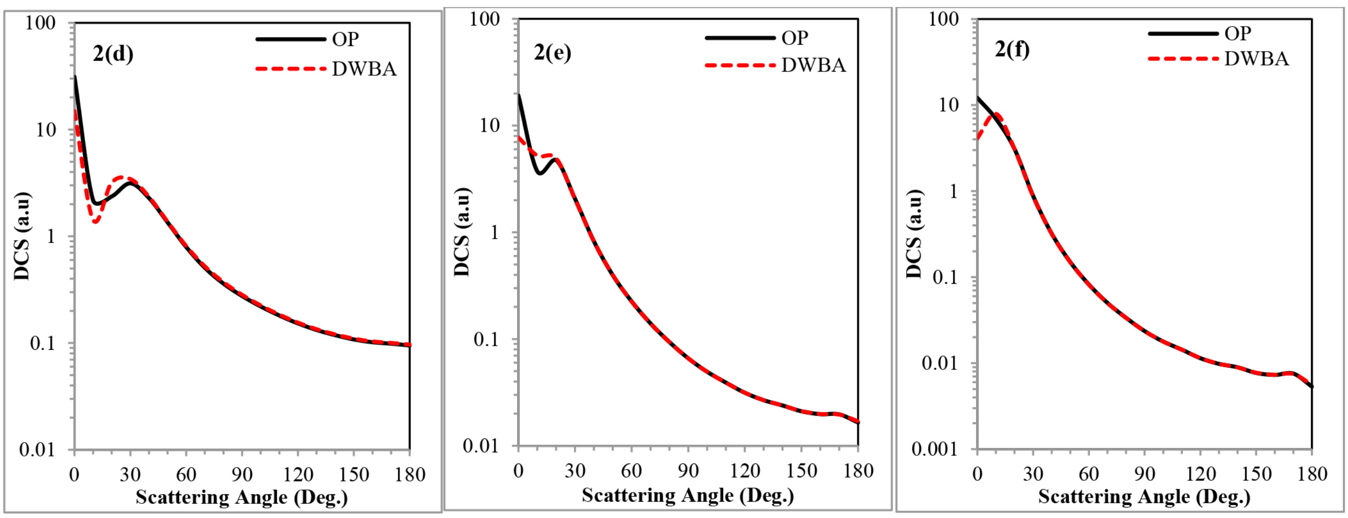


**Fig. 2(d)**, **2(e)** and **2(f)**: Same as **Fig. 2(a)** but respectively at 30.0 eV, 100.0 eV and 200.0 eV

## Electron-Beryllium Total Cross Section (TCS) and Elastic Cross Section (TECS)

In **fig. 3**, the OP_Present TECS results agree well with the relativistic calculations of McEachran *et al.* (2018) which overestimates the DWBA_Present data by $\approx 10.78\%$ at impact energies $45 \le E \le 200$ eV. The 1997 convergent close-coupling calculations of Fursa snd Bray and their recent work with Zatsarinny and Bartschat (2016) respectively underestimates the DWBA_Present data by $\approx 6.64\%$ for $105 \le E \le 200$ eV and $\approx 10.64\%$ for $20 \le E \le 100$ eV. Similarly, the Reid and Wadehra (2020) OP results underestimates the DWBA_Present data by $\approx 6.64\%$ at $105 \le E \le 200$ eV. The disparity in results is due to the application of several distinct model potentials to account for the diverse physical effects of electron scattering by beryllium atoms.

In **fig. 4**, the present TCS OP and DWBA results are respectively denoted by OP_e and DWBA_e, while R and W, Z *et al.* and F and B respectively denote the calculations of Reid and Wadehra (2020), Zatsarinny *et al.* (2016) and Fursa and Bray (1997).

The agreement among OP_e, DWBA_e and F and B is excellent. Further, there is very good agreement between the present calculations and the results of R and W save for the interval $55 \le E \le 175$ eV where R and W overestimates DWBA_e and OP_e respectively by $\approx 4.963\%$ and $\approx 2.963\%$. The Z *et al.* results slightly underestimates the present data. All the data show a drop with increasing impact energy, suggesting a decrease in scattering likelihood due to shorter projectile-target interaction time.

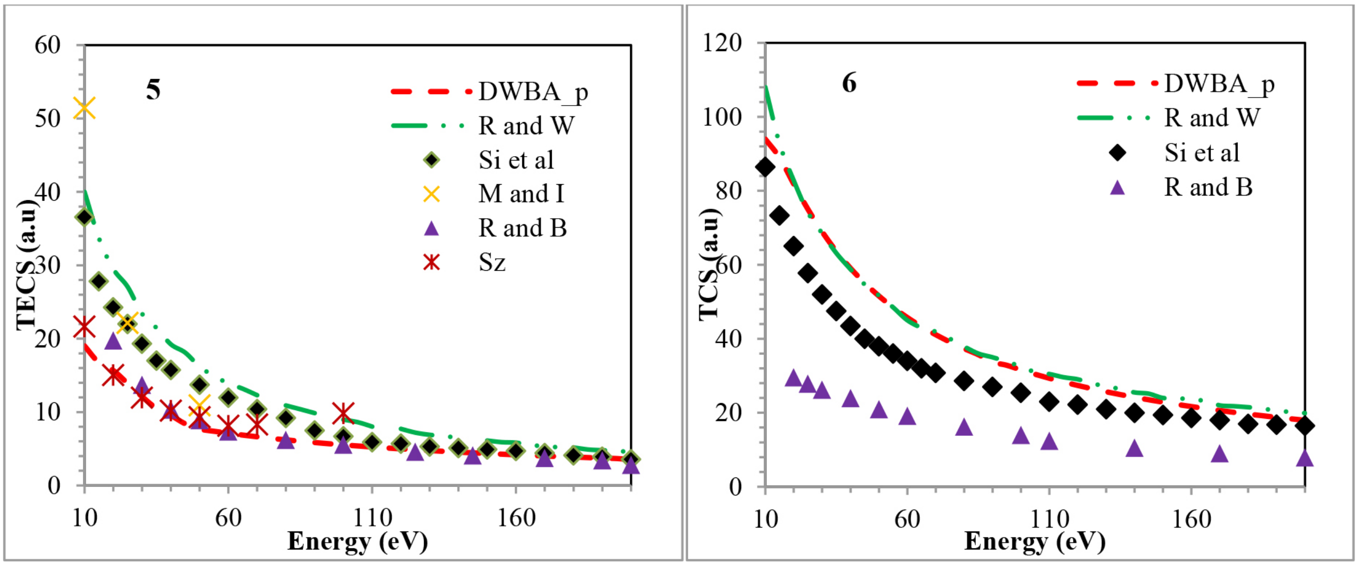


**Fig. (3)** and **(4)**: Respectively Electron - Beryllium TECS and TCS at impact energies $5 \le E \le 200$ eV.

## Positron-Beryllium Total Cross Section (TCS) and Elastic Cross Section (TECS)

In **fig. 5**, the present TECS dataset is denoted by DWBA_p, while the calculations of Reid and Wadehra (2020), Singh *et al.* (2018), Mitroy and Ivanov (2002), Raizada and Baluja (1996) and Szmytkowski (1993) are respectively represented by R and W, Si *et al.*, M and I, R and B and Sz.

At impact energies $E \le 100$ eV, the data show markedly distinct tendencies. For the available data, the trends are consistent for $E \ge 100$ eV. This is not surprising given that at such high energies, the cross sections depend less on the interaction potential and more on the kinetic energy of the projectile.

In **fig. 6**, the present TCS dataset is denoted by DWBA_p, while the calculations of Reid and Wadehra (2020), Singh *et al.* (2018), Raizada and Baluja (1996) are respectively represented by R and W, Si *et al.* and R and B.

The present results agree quite well with the calculations of R and W. DWBA_p and Si *et al.* agrees fairly well for $E \ge 135$ eV but the later underestimates the former for $E < 135$ eV. Although R and B exhibit similar trend as DWBA_p, the former greatly underestimates the later. This is expected since R and B utilized the empirical factor, $\left[(kr)^{-1}\right]^{1/2}$, to account for positronium formation. At 10 eV, their TECS = TCS = 15 Å suggesting zero absorption cross section yet beryllium's Ps-formation threshold $\approx 2.523$ eV implying TCS is expected to be more than TECS at $E = 10$ eV. R and B thus inadequately handled Ps-formation hence the difference between their results and our present data.

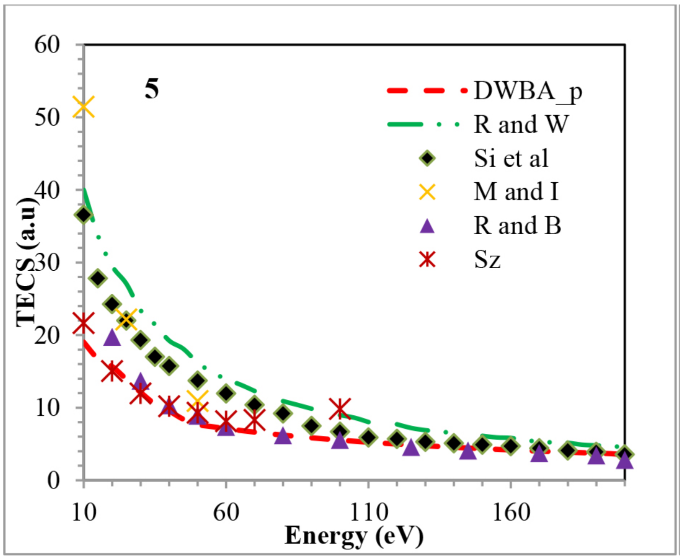


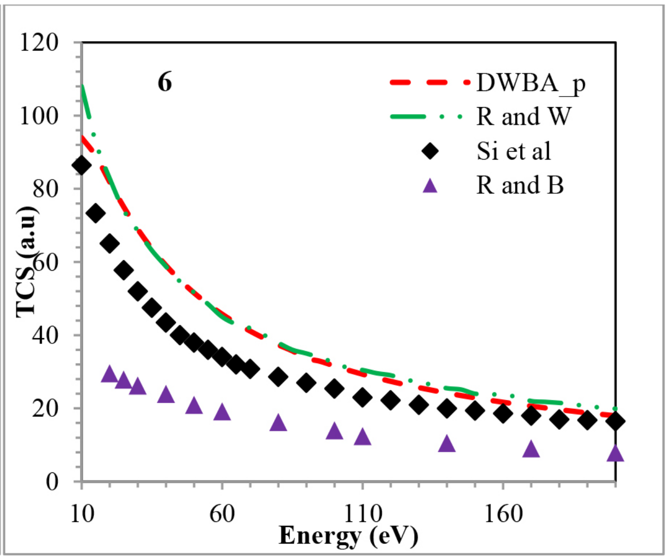


**Fig.** **(5)** and **(6)**: Respectively Positron - Beryllium TECS and TCS at impact energies $10 \le E \le 200$ eV.

**Electron- and Positron-Beryllium Momentum Transfer Cross Section (MTCS)**

**Fig.** **(7)** and **(8)** are respectively the electron_beryllium and positron_beryllium momentum transfer cross sections. In fig (7), the present MTCS agrees fairly well with the McEachran *et al.* (2018) results but overestimates the Reid and Wadehra (2020) results by about an order-of-magnitude at $10 \le E \le 100$ eV. In fig (8), the present MTCS exhibit similar trend in shape and structure with the data of Reid and Wadehra (2020) save that the later underestimates the present results by a factor of $\approx 0.8$. The reason for large discrepancy between Singh *et al.* (2018) and our results remains unclear although the Singh *et al.* (2018) results are somewhat unusual since one would expect that at high energies $\sigma_{mtcs} < \sigma_{el}$ which, from their results, is not the case.

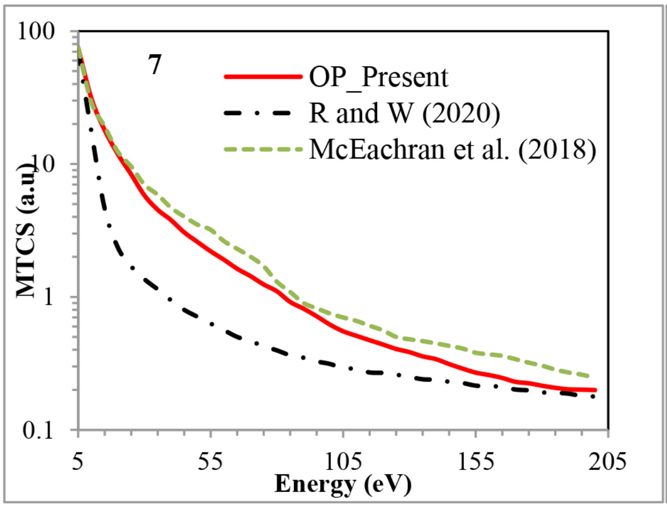


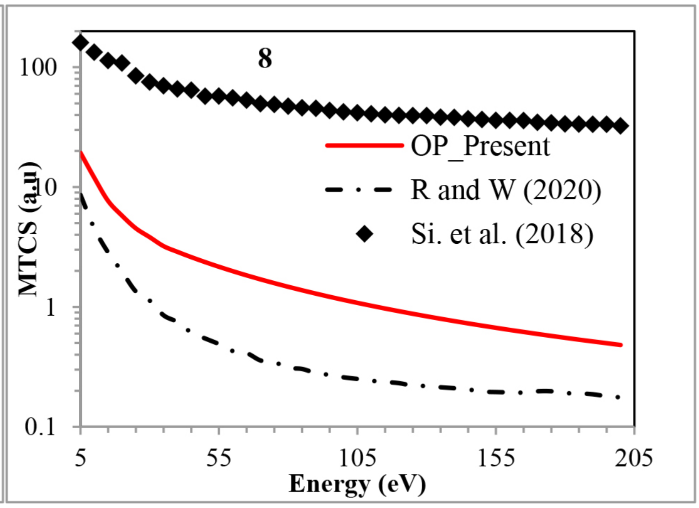


**Fig.** (7) and **(8)**: Respectively electron_beryllium and positron_beryllium MTCS at impact energies $5 \le E \le 200$ eV.

## CONCLUSIONS

We have applied both the first order distorted wave Born approximation and the optical potential method with a complex potential to calculate DCS, TECS and TCS. With a complex potential, the agreement between the present OP and DWBA and other available DCS results is quite good. This affirms the minor influence of the DWBA T-matrix's second direct term (equation 3) on DCS values. The positronium formation channel slightly increases the total cross sections at $E \le 150$ eV. Its effect on the cross sections beyond 150 eV is negligible since the positronium formation channel extends from the positronium formation threshold to $\approx 150$ eV. Noting the practical applications of electron- and positron-atomic beryllium scattering cross sections, experimental data would be of significant value in resolving the discrepancy among available theoretical data.

## Author Contributions

Kariuki P. K. conceptualized the project, developed the electron-magnesium atom elastic scattering code and supervised the project. Wechuli W. B. modified the code, performed the calculations, gathered the data and wrote the manuscript. Linturi J. M. supervised the project, read and commented on the manuscript. Waswa V. E. prepared the graphical abstracts. All authors developed the underlying theoretical techniques and discussed the results.

## Compliance with Ethical Standards

**Funding:** Not applicable; authors did not receive any external financial support for this research.

## Declarations

**Conflict of Interest:** The authors declare no competing interests.

**Data Availability Statement:** This manuscript has no associated data or the data will not be deposited. All the data reported herein is available upon reasonable request through the corresponding author's e-mail.
**Ethical Approval:** The manuscript has not been published and is not being submitted or considered for publication elsewhere. The text, illustrations and any other materials included in the manuscript do not infringe upon any existing copyright or other rights of anyone.

## REFERENCES

Bunge, C. F., Barrientos, J. A., and Bunge, A. V. (1993). Roothan-Hartree-Fock Ground State Atomic Wave Functions: Slater-Type-Orbital Expansions and Expectation values for $Z = 2 - 54$. *Atomic Data and Nuclear Data Tables.* **53,** 113-401.

Chiari, L., Zecca, A., Girardi, S., Trainotti, E., Blanco, F., McEachran, R. P., and Brunger, M. J. (2012). Positron Scattering from $O_2$: *Journal of Physics B: Atomic, Molecular and Optical Physics* **45**(21)215206. URL http://dx.doi.org/10.1088/0953-4075/45/21/215206

Furness, J.B. and McCarthy, I.E. (1973). Semiphenomenological Optical Model for Electron Scattering on Atoms. *Journal of Physics. B:* **6**, 2280 – 2291.

Fursa, D., and Bray, I. (1997). Bayesian atomic structure calculations for collisional problems. *Journal of Physics B:* **30**, L273

Fursa, D.V., and Bray, I. (2012). Convergent Close-Coupling Method for Positron Scattering from Noble Gases. New Journal of Physics. 14, 035002 (18 pp).

Kaushik, Y. D., Khare, S. P., and Kumar, A. (1983). Critical points for electron-beryllium elastic scattering. *Journal of Physics B: Atomic, Molecular and Optical Physics* **16** (1983) 3609-3619

Khare, S. P., Kumar, A., and Vijayshri, K. V. (1985). Elastic scattering of Electrons and Positrons by Ca atom. : *Journal of Physics B: Atomic, Molecular and Optical Physics* **18** (9) 1827-1840. https://stacks.iop.org/0022-3700/18/i=9/a=016

McEachran, R. P., Blanco, F., Garcia, G., and Brunger, M. J. (2018). A relativistic complex optical calculation for electron-beryllium scattering. *J. Phys. Chem.* Ref. Data **47**, 033103. https://doi.org/10.1063/1.5047139

Mitroy, J., and Ivanov, I. (2002). Semiempirical model of positron scattering and annihilation. *Phys. Rev.* A **65,** 042705

Raizada, R., and Baluja, K. L. (1996). Positron Scattering from alkaline-earth elements, Pramana **47** (1) 87-98. URL http://dx.doi.org/10.1007/BF02847169

Reid, D. D., and Wadehra, J. M. (2020). Electron and positron scattering by atomic beryllium. *The European Physical Journal D.* **74** (112). https://doi.org/10.1140/epjd/e2020-100221-3

Savage, J. S., Fursa, D. V., and Bray, I. (2012). Convergent close-coupling calculations of positron-magnesium scattering, *Phys. Rev.* A 83 062709. URL https://link.aps.org/doi:10.1103/PhysRevA.83.062709

Singh, S., Anamika, S., and Bobby, A. (2018). Positron scattering calculations of elastic, total and momentum transfer cross sections for alkaline earth atoms. *International Journal of Mass Spectrometry* 428 pp 22-28. https://doi.org/10.1016/j.ijms.2018.02.005

Staszewska, G., Schwenke, D. W., Thirumalai, D., and Truhlar, D. G. (1983). Quasifree-scattering model for the imaginary part of the optical potential for electron scattering. *Physical Review.* A **28** 2740-2751. URL https://link.aps.org/doi/10.1103/PhysRevA.28.2740

Szmytkowski, R. (1993). Theoretical study of low-energy positron scattering on alkaline-earth atoms in the relativistic polarized orbital approximation. *Journal of Physical II France* **3**(2) (1993) 183-189. https://doi.org/10.1051/jp2:1993120

Utamuratov, U., Fursa, D. V., Kadyrov, A. S., Lugovskoy, A. V., Savage, J. S., and Bray, I. (2012). Two-center convergent-close-coupling calculations of positron scattering on magnesium. *Phys. Rev.* A **86**, 062702. URL https://link.aps.org/doi:10.1103/PhysRevA.86.062702

Wechuli, W., Linturi, J., and Kariuki, P. (2022). Positron impact elastic scattering by calcium atom using first order distorted wave born approximation with a complex potential. *African Journal of Pure and Applied Sciences,* 3(1), 177-184. https://doi.org/10.33886/ajpas.v3i1.261

Wisniewski, E., Conde, M., Gai, W., Ha, G. and Power, J. (2015). Multiple scattering effects of a thin beryllium window on a short, 2 nC, 60 MeV Bunched Electron Beam, in *proceedings, 6th International Particle Accelerator Conference (IPAC 2015): Richmond, Virginia, USA, 3-8 May 2015*, p. WEPTY012.

Zatsarinny, O., Bartschat, K., Fursa, D. V., and Bray, I. (2016). Calculations for electron-impact excitation and ionization of beryllium. *J. Phys. B: At. Mol. Opt. Phys*. **49**, 235701. https://doi.org/10.1088/0953-4075/49/23/235701

Zatsarinny O. and Bartschat K. (2013). The B-spline R-matrix Method for Atomic Processes: Application to Atomic Structure, Electron Collisions and Photoionization. *J. Phys. B: At. Mol. Opt. Phys*. **46**, 112001. https://doi.org/10.1088/0953-4075/46/11/112001